Structural Forces from Directed Self-Assembly†

Panagiotis Angelikopoulos, Saud Al Harthy, and Henry Bock*

Department of Chemical Engineering, Heriot-Watt University, Edinburgh, EH14 4AS, Scotland, U.K.

Received: April 4, 2009; Revised Manuscript Received: May 29, 2009

We investigate a candidate structure for the bottom-up design of nanocomposite materials. At a pair of crossing carbon nanotubes, surfactants self-assemble into a micelle-like aggregate incorporating the two tubes. The aggregate forms as long as the gap between the tubes is smaller than the core diameter of a bulk micelle. Moreover, the absorbed surfactant aggregate generates an effective force between the tubes. The dependence of this force on the distance between the tubes is complex and includes structural components, such as layering, and a large attractive region at larger distances. This attraction appears to be entropic in nature and to originate from confinement of the surfactant head groups.

Introduction

Self-assembly and particularly directed self-assembly of amphiphilic molecules are promising candidates for the bottom-up manufacture of advanced nanostructured materials. Their key advantage is the autonomous formation of a number of nanoscale structures that can be controlled to some extent by macroscopic parameters such as the bulk amphiphile concentration. To use these processes effectively, it is necessary that they are well understood.

Surfactant self-assembly has been widely studied in the past experimentally,[1,2] theoretically,[3] and using computer simulations.[4,5] Also, their aggregation behavior in the presence of solid surfaces[6−8] and in pores[9−11] has been investigated. However, for bottom-up techniques, understanding of surfactant self-assembly on nanoparticles is critical. Their high mean curvature distinguishes self-assembled surfactant aggregates from other materials and leads to structures that would not be possible otherwise, e.g., spherical micelles incorporating a thin hydrophobic carbon nanotube.[7,12,13]

An entirely new aspect comes into play when these self-assembled structures are to be used to synthesize nanocomposite materials. In this case, it is relevant to understand how the self-assembled aggregates influence the material's structure. Thus, knowledge of the surfactant mediated interactions between the other constituents of the material is relevant.

Particularly interesting building blocks are carbon nanotubes (CNTs). The direct interactions between carbon nanotubes are dominated by van der Waals (VdW) interactions if they are in vacuum. Using spectroscopic methods, O'Connell et al.[14] experimentally estimated the binding energy for two nanotubes in a bundle to be approximately 500 eV/μm of tube/tube contact. VdW forces between tubes have also been investigated theoretically. Schroder et al.[15] and Kleis et al.[16] have used a density functional theory (DFT) approach to estimate the interaction strength between parallel and concentric nanotubes. Their results suggest that the binding energy is radius dependent with larger tubes having a larger binding energy per tube. For a pair of tubes of 0.4 nm radius, they find a binding energy of approximately 1500 eV/μm of tube length at a tube/tube separation of 0.552 nm. Girifalco et al.[17] use both DFT and an empirical model to estimate the van der Waals binding energy between tubes and found approximately 1000 eV/μm of tube/tube contact at room temperature.

As carbon nanotubes are hydrophobic, solvent mediated (hydrophobic) forces are expected in (aqueous) solution.[18] The ratio between VdW and the hydrophobic contribution, to our knowledge, has not been measured experimentally. Walther et al.[19] performed fully atomistic molecular dynamics simulations of single wall carbon nanotubes in SPC water. They calculate potentials of mean force for the interaction between (16,0) tubes of radii 0.5−0.6 nm. The computed mean force exhibits an attractive maximum at a tube spacing of 0.5 nm which corresponds to approximately one unstable layer of interstitial water molecules. The authors find that the van der Waals attraction between the carbon surfaces is the dominant force by comparing their solution results to simulations of the system in vacuum. The authors estimate a tube/tube binding energy, including both VdW and hydrophobic contributions of 850 eV/μm at a tube spacing of 0.56 nm.

While these results deviate significantly from each other, they indicate that strong interactions between the tubes are rather short ranged. They also suggest that the interactions between carbon nanotubes in aqueous solution might be dominated by van der Waals interactions.

Here, we employ computer simulations to study the forces exerted by surfactant molecules on a pair of crossing carbon nanotubes. The two nanotubes cross at a right angle, and a surfactant micelle is formed incorporating the crossing (Figure 1). This situation can be achieved by adjusting the bulk concentration such that the higher hydrophobic potential at the crossing due to the presence of two surfaces leads to predominant adsorption and self-assembly at the crossing.[7] The distance dependence of the effective force between the tubes generated by the surfactant aggregate is very rich. It is dominated by a large attractive region; i.e., the adsorbed self-assembled surfactant aggregate stabilizes the crossing.

Model and Simulation

The same model and simulation methodology has been used before;[7] therefore, we describe it only briefly.

Model. Surfactant molecules (H_5T_5) are represented as a chain of five hydrophilic head (H) beads followed by five hydrophobic tail (T) beads. The solvent is treated implicitly. This and the

† Part of the "H. Ted Davis Special Section".

* To whom correspondence should be addressed. E-mail: h.bock@hw.ac.uk.

10.1021/jp903121a CCC: $40.75
Published on Web 07/14/2009

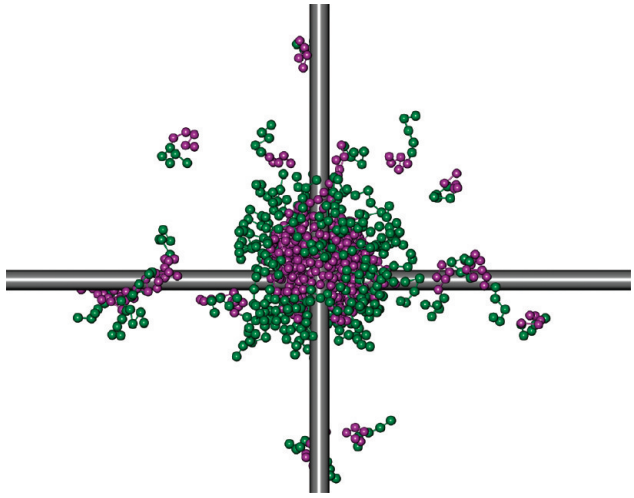

Figure 1. Surfactant molecules adsorb and self-assemble into a "central aggregate" at a pair of carbon nanotubes. At the appropriate thermodynamic conditions, a central aggregate is formed, while most of the tubes' surface area remains empty. Here, the distance between the axis of the tubes is $d_{CNT} = 2.5\sigma$. Hydrophobic beads are shown in purple, while hydrophilic beads are colored green.

coarse-grained character of the surfactant beads causes the beads to interact via effective potentials. Here, we employ a common empirical model, where the interaction between hydrophobic beads is attractive, while all other bead/bead interactions are repulsive. The force shifted Lennard-Jones (LJ) (12,6) potential $\phi(r_{ij})$ is used to represent attractive interactions between beads i and j

$$\phi_{LJ}(r_{ij}) = 4\varepsilon\left[\left(\frac{\sigma}{r_{ij}}\right)^{12} - \left(\frac{\sigma}{r_{ij}}\right)^{6}\right] \tag{1}$$

$$\phi(r_{ij}) = \begin{cases} \phi_{LJ}(r_{ij}) - \phi'_{LJ}(r_{cut})(r_{ij} - r_{cut}) - \phi^{LJ}(r_{cut}) & r_{ij} < r_{cut} \\ 0 & r_{ij} \geq r_{cut} \end{cases} \tag{2}$$

where r_{cut} is the cutoff radius, $\phi'_{LJ}(r) = d\phi_{LJ}(r)/dr$, $r_{ij} = ||\mathbf{r}_{ij}||$, $\mathbf{r}_{ij} = \mathbf{r}_j - \mathbf{r}_i$, and $\mathbf{r}_i$ and $\mathbf{r}_j$ are the positions of i and j, respectively; ε is the well depth and σ the length parameter of the LJ potential. Repulsive interactions are modeled using the WCA potential given by eq 2 with $r_{cut} = 2^{1/6}$. Beads k and l which are nearest neighbors in a chain additionally interact via the harmonic bond potential $\phi_{bond}(r_{kl}) = \varepsilon_{bond}(r_{kl} - r_{bond})^2$, where ε_{bond} is the depth of the potential well and r_{bond} the bond length.

At the level of coarse graining of the surfactant molecules, CNTs are smooth cylinders. Here, we model their interactions with hydrophobic surfactant beads via the force shifted Lennard-Jones (12,6) potential in eq 2 which is also shifted to the surface of the nanotubes

$$\phi_{CNT}(r_i) = \frac{\varepsilon_{CNT}}{\varepsilon}\phi(r_i - r_{CNT}) \tag{3}$$

where r_i is the shortest distance[20] between bead i and the nanotube axis and r_{CNT} is the radius of the nanotube. Repulsive interactions with the hydrophilic head beads are modeled using the WCA potential, i.e., $\phi_{CNT}(r_i)$ with $r_{cut} = 2^{1/6}$. All potential parameters can be found in Table 1.

TABLE 1: Model and Simulation Parameters in Reduced Units

surfactants	T beads = 5	H beads = 5
	$\varepsilon = 1.0$	$\sigma = 1.0$
	$\varepsilon_{bond} = 4.0$	$\sigma_{bond} = 1.2$
nanotubes	$r_{CNT} = 1.0$	$d_{CNT} = 2.0-10.0$
		$\varepsilon_{CNT} = 2.5$
simulation	$T = 0.7$	$\Delta t = 0.005$
	attractive: $r_{cut} = 2.5$	repulsive: $r_{cut} = 2^{1/6}$
	nonconservative: $r_{cut} = 2.5$	DPD: $\xi = 1.0$
	chains = variable	production = $0.5 \times 10^8 \Delta t$
	elongated box = $100 \times 100 \times 200$	equilibration = $(1-2) \times 10^8 \Delta t$

Simulation. We investigate the system in the canonical ensemble using the dissipative particle dynamics (DPD) method.[21] In DPD, any two particles i and j interact via the pairwise force $F_{ij} = F_{ij}^C + F_{ij}^R + F_{ij}^D$, where F_{ij}^C, F_{ij}^R, and F_{ij}^D are the conservative, random, and dissipative forces, respectively. The random force is given as

$$F_{ij}^R = \begin{cases} -\xi\omega^R(r_{ij})\theta_{ij}\hat{\mathbf{r}}_{ij} & r_{ij} \leq r_{cut} \\ 0 & r_{ij} > r_{cut} \end{cases} \tag{4}$$

where $\hat{\mathbf{r}}_{ij} = \mathbf{r}_{ij}/||\mathbf{r}_{ij}||$, ξ is the strength parameter, and θ_{ij} is a random variable with limits of -1 and 1, and zero mean (see ref 22 for the utilized random number generator), while the dissipative force is

$$F_{ij}^D = \begin{cases} -\gamma\omega^D(r_{ij})(\hat{\mathbf{r}}_{ij}\cdot\mathbf{v}_{ij})\hat{\mathbf{r}}_{ij} & r_{ij} < r_{cut} \\ 0 & r_{ij} > r_{cut} \end{cases} \tag{5}$$

where γ is the strength parameter. It is important to recognize that F_{ij}^R is a stochastic force which requires slight modifications of the integration algorithm.[21]

In the canonical ensemble, the dissipative and random forces are connected by the fluctuation dissipation theorem leading to

$$\begin{aligned} \omega^D(r_{ij}) &= [\omega^R(r_{ij})]^2 \\ \xi^2 &= 2\gamma k_B T \end{aligned} \tag{6}$$

where k_B is Boltzmann's constant and T is the temperature. Thus, the random and dissipative forces together constitute the DPD thermostat. Here, we use the weight functions originally published in ref 21

$$\omega^D(r_{ij}) = \begin{cases} (1 - r_{ij}/r_{cut})^2 & r_{ij} < r_{cut} \\ 0 & r_{ij} > r_{cut} \end{cases} \tag{7}$$

where we have chosen $\omega^D(r)$ to be of the same range as the attractive conservative force.

As the bulk surfactant concentration is not one of the natural parameters of the inhomogeneous canonical ensemble, it can not be preset. Therefore, it has been maintained in the initial part of the equilibration period by insertion and deletion of surfactant molecules if the actual concentration in the bulk-like region deviates by more than 5% from the target. Because the concentration might change somewhat during the remaining equilibration time, the resulting average concentrations for the individual simulations fluctuate within about 10% of the target value of $C = 1.5 \times 10^{-5}$. This keeps the concentration well in the range where the target structures are expected.[7] We have

further confirmed that none of the quantities of interest correlate with the random deviations of the actual concentration.

In all simulations, an elongated box is used to provide a bulk-like region for concentration control and the usual periodic boundary conditions are employed. Further details of the simulation protocol can be found in ref 7.

Reduced Units. Throughout, we use reduced quantities: lengths are given in units of the LJ length parameter σ, the energy is scaled with the well depth of the bead/bead LJ interaction ε, the temperature scale is given in terms of ε/k_B, and time is represented in units of $(m\sigma^2/\varepsilon)^{1/2}$, where m is the mass of a bead. Concentrations are defined as molecular number densities and given in units of $1/\sigma^3$.

Results and Discussion

We study the effect of surfactant adsorption on the force between carbon nanotubes. Here, we are interested in the situation where two tubes cross at a right angle and the bulk surfactant concentration $C = 1.5 \times 10^{-5} \approx 0.3C_{CMC}$ is chosen such that adsorption and aggregation occur predominantly at the crossing.[7] As shown in Figure 1, adsorbed surfactant molecules self-assemble into a micelle-like central aggregate.

The surfactants in the central aggregate interact with the tubes which can create a net force acting on each tube. As all forces must be balanced and the two tubes are the only fixed objects in the system, the forces on the tubes must be equal in magnitude and opposite in direction. Thus, surfactants create an effective force between the tubes. It is also possible to view this from a different perspective: If an external force is applied to one of the tubes, it is mediated by the surfactants to the other tube.

Because of the symmetry of the crossing, the total force exerted by the surfactants on the nanotubes can only act along the direction perpendicular to both tube axes which we define to be the z-direction. Indeed, all simulation results show that the x- and y-components of the average force on the tubes are zero (results not shown). Therefore, only the z-components of the individual bead/CNT interactions contribute to the surfactant generated force between the CNTs.

In the canonical ensemble, this force between the tubes is defined as

$$F = \langle \sum_{i=1}^{N} \sum_{k=1}^{10} f_z(i,k) \rangle \qquad (8)$$

where $f_z(i,k)$ is the z-component of the force exerted by bead k in chain i on the nanotube, $\langle ... \rangle$ denotes the canonical ensemble average, the first sum runs over all N surfactant molecules, and the second over all 10 beads in the respective chain.

To analyze the surfactant generated force, we simulate a number of independent systems with tube/tube distances from $d_{CNT} = 2$ to 10 and determine the forces between the tubes. The resulting force−distance curve is presented in Figure 2a. One immediately observes four key features: (i) an initial repulsive region, (ii) decaying oscillations, (iii) an attractive region, and (iv) a jump to negligible forces at $d \approx 7.5$.

At $d \approx 7.5$, the central aggregate ruptures, leaving only relatively few surfactant molecules adsorbed along the tubes. The majority of the adsorbed molecules form small aggregates on each of the tubes independently (Figure 3). Therefore, the curve representing the aggregation number of the central aggregate, shown in Figure 2b, ends at $d \approx 7.5$. The vanishing of the force between the tubes at $d \gtrsim 7.5$ is, therefore, not surprising. It is also not surprising that the central aggregate

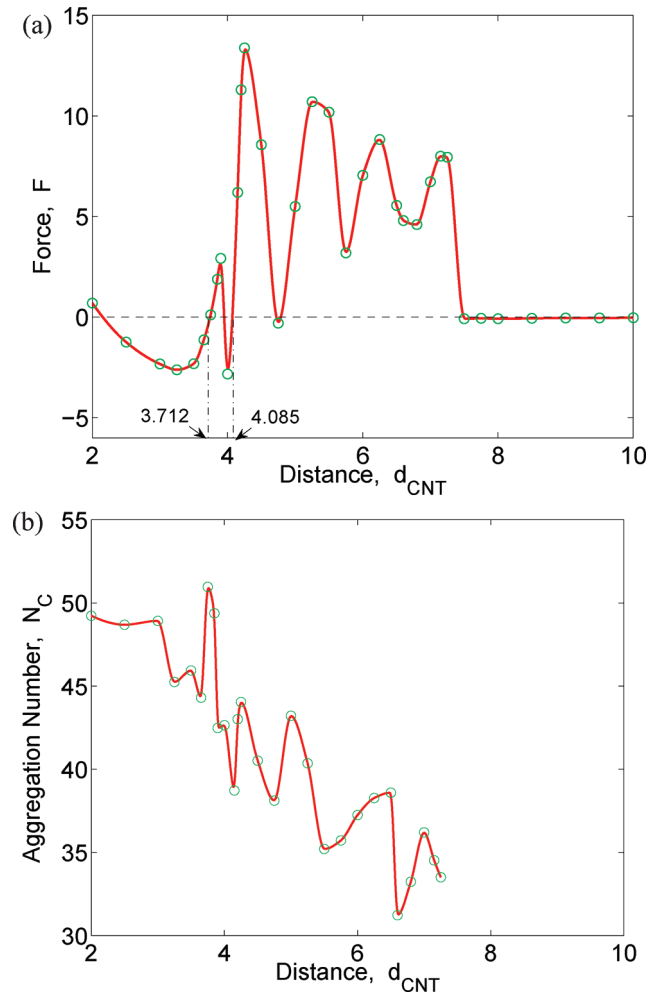

Figure 2. Distance dependence of (a) the force between the carbon nanotubes generated by the adsorbed surfactant aggregate and (b) the number of surfactant molecules forming the aggregate. The solid lines are guides to the eye. For comparison, the aggregation number of bulk micelles just above the critical micelle concentration (CMC) is approximately 41 molecules.

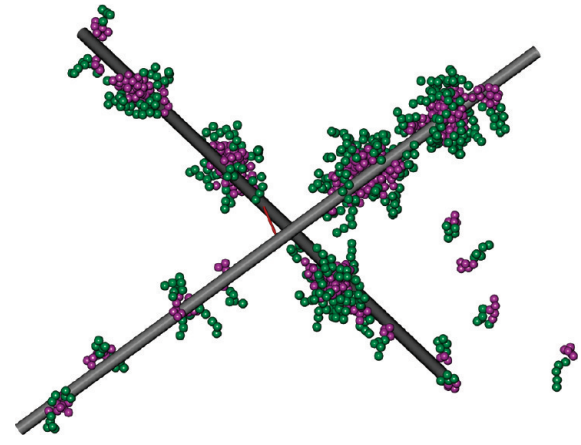

Figure 3. At too large tube/tube distances, the central aggregate is not formed. Here, $d_{CNT} = 9.0$. The red line indicates the center of the crossing where the central aggregate would be expected to form at smaller distances.

disappears at large tube/tube separations. The high hydrophobic potential due to the presence of two hydrophobic surfaces near the crossing leads to the formation of the central aggregate at a concentration where the remaining tube surface cannot stabilize large aggregates. As the distance between the tubes is

increased beyond $d \approx 7$, the distance between the tube surfaces becomes larger than the average core diameter of the bulk micelles[7] $D \approx 5$. Thus, to significantly benefit from interactions with both tubes, the micelle is stretched. Finally, the gap is too large to be bridged by the micelle. At $d \approx 7.5$, the two tubes become independent.

To interpret the surfactant/nanotube force at lower distances between the nanotubes, it is essential to understand in detail how it is generated. A single independent hydrophobic bead that adsorbs onto a carbon nanotube would be located in the global minimum of the bead/CNT potential. In this situation, there are no forces acting on the particle or, equivalently, on the carbon nanotube. If we postulate an "auxiliary" force acting on the bead in the radial direction, then the bead will be pushed or pulled out of the bead/nanotube potential minimum until the forces are again balanced. This creates a force between the tube and the bead. If the auxiliary force does not point in the radial direction, then there are force components which are not balanced by the interaction with the nanotube.

Considering a carbon nanotube positioned such that its axis coincides with the x-axis, one can identify a number of extreme cases. Because of the radial direction of the bead/CNT interaction, a particle located in the xy-plane, i.e., $z = 0$, cannot generate a force component in the z-direction. On the other hand, a particle in the xz-plane would have a z-component of the force only. In between these two extreme cases, the angle between the z-axis and the bead/tube force vector decreases from $\pi/2$ to 0 as we move from the xy- to the xz-plane and, consequently, the z-component of the force increases.

The forces on a bead interacting with two tubes must be balanced as well. Thus, the force between one tube and the bead must be "relayed" to the other one through other beads or, most importantly, through direct interaction with the second tube. For direct mediation of a force in the z-direction, the particle must have a z-component of the force with each of the tubes simultaneously. The rapid decrease of the bead/CNT force with increasing bead/CNT distance prompts us to assume that the mediated force is dominated by beads that are simultaneously near both tubes. These are beads located near the global minimum of the bead/CNT potential. We will show later that the density of hydrophobic beads is very high in this region, emphasizing its importance.

We now return to the analysis of the force curve. At the smallest tube/tube separations, the surfactant generated force between the tubes is repulsive; its magnitude initially increases, goes through a repulsive maximum, and decreases again. To analyze the origin of this behavior, computer simulations have the great advantage that they provide insight into the internal structure of the central aggregate. To investigate this internal structure, it is represented by local density maps and density isosurfaces in Figure 4. The local density maps are shown for a plane that cuts through the center of the central aggregate; the plane is perpendicular to the upper tube and parallel to the lower tube.

The local density maps for tube/tube distances $d_{CNT} = 2.00$, 3.25, and 3.75 shown in Figure 4b, d, and f reveal that the density of hydrophobic beads is high at positions close to the nanotubes. This is caused by the high hydrophobic-bead/CNT interaction. These regions of high density indicate the position of the potential minimum. The potential minimum for each individual tube forms a cylindrical surface with radius $r_{tube} + 2^{1/6}$. As the potentials are additive, the intersection line of the two cylindrical surfaces represents the global potential minimum of the crossing. We expect the density to be highest in the global potential minimum, as in this position beads can interact with both tubes simultaneously. This is visible in Figure 4b where the position of the global minimum is indicated by the arrow. The deformed torus in Figure 4a demarcates the location of highest density in the system and simultaneously the location of the global potential minimum. Consequently, particles in this torus are likely to dominate the effective force between the tubes.

The magnitude of the surfactant generated force between the tubes depends on three factors: (i) the number of particles directly interacting with the two tubes, (ii) the relative size of their force z-component, i.e., the angle between the total force and the z-direction, and (iii) the magnitude of the total bead/CNT force.

As is clearly shown in the sequence of density isosurfaces in Figure 4, the length of the deformed torus indicating the location of beads near the global potential minimum shrinks with increasing distance between the tubes. Since the density in this region is approximately constant (Figure 4), the number of beads in the torus is approximately proportional to its length. Thus, the number of beads interacting with both tubes simultaneously decreases with increasing CNT/CNT distance. The dependence is nonlinear; it is slow initially and becomes faster as the distance increases.

A bead near the global potential minimum is surrounded by other beads. These beads are located in the attractive range of the bead/CNT potential which pulls them toward the tubes. This generates a force pushing the first bead out of the potential minimum into the repulsive region of the potential. The general direction of this pushing force is toward the center of the crossing. Like a wedge, the hydrophobic beads are pulled in between the tubes. As the attractive region of the total bead/CNT potential does not change too much in the considered region of tube/tube distances, we assume that the "push" is approximately constant.

Following again the picture of the wedge, it becomes clear that for a constant pushing force the z-component of the responding bead/CNT repulsion becomes larger the smaller the angle between the z-component and the pushing force is. Although not all positions in the torus are identical, this angle generally increases as the beads move into the center of the crossing. Thus, the force in the z-direction increases as the distance between the tubes increases. This continues until the reduction in the number of force mediating beads overcompensates the effect and the force starts to decrease again, creating a repulsive maximum (Figure 2a).

At distances $d \gtrsim 3.5$, the torus is short enough that the particles in it start to correlate. The potential energy of the beads in the torus is minimal if they are located in the global minimum of the bead/CNT potential and simultaneously in the minimum of the bead/bead potentials. For a torus consisting of eight beads, one can calculate the optimal tube/tube distance to be $d_{CNT} = 3.712$. A bead located in the potential energy minimum does not exert a force on the nanotubes. The force curve in Figure 2a indicates a zero in the force very near the predicted point.

As discussed above, beads surrounding the inner torus push beads located in the torus toward the region between the tubes. Because the particles in the torus are now correlated and interact strongly with each other, this push does not need to be compensated by the bead−nanotube interactions but is compensated by a slight compression of the torus. As a consequence, the zero in the force would be expected at tube/tube separations slightly larger than the "undisturbed" prediction of $d_{CNT} = 3.712$.

Because of the symmetry of the system, another zero in the force is expected for a torus consisting of four hydrophobic

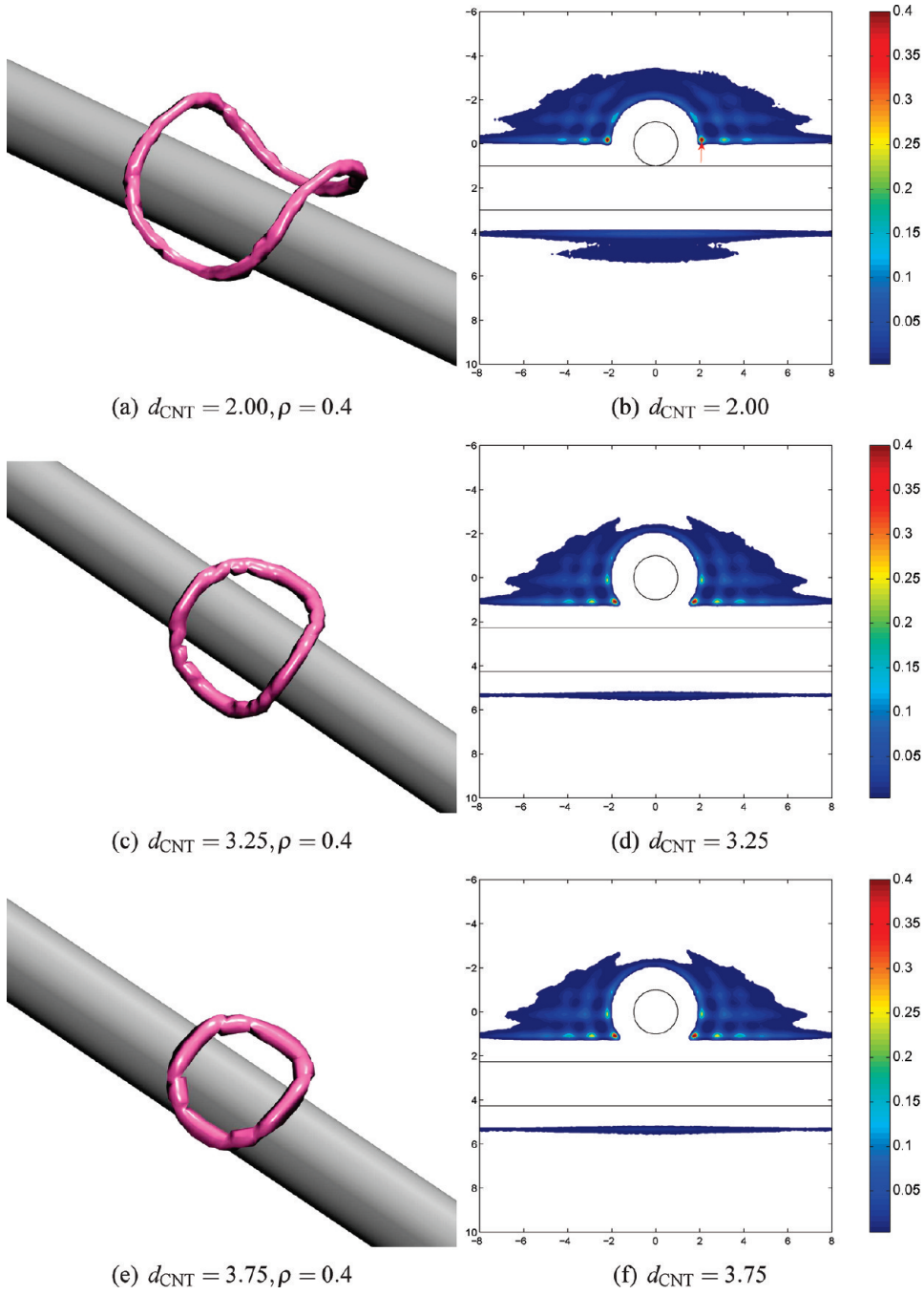

Figure 4. Details of the internal structure of the hydrophobic core of the central aggregate in the repulsive force regime at three distances between the tubes d_{CNT} as indicated in the figure: (left column) density isosurfaces for $\rho = 0.4$ with the upper tube removed for clarity; (right column) local density maps for a plane through the center of the crossing, parallel to the lower tube and perpendicular to the upper tube. The arrow in part b indicates the point of highest bead/CNT potential where beads are in the potential minimum of both tubes simultaneously. Note the diminishing length of the torus of highest density with increasing d_{CNT}.

beads. Following the same arguments detailed above, one obtains $d_{CNT} = 4.089$ as the predicted location of the zero. This result is again consistent with the force curve in Figure 2a.

Between the two zeros, the force initially becomes attractive, goes through a maximum, then becomes repulsive after going through another zero, and reaches a repulsive maximum before approaching zero again. The natural response of a stable state to distortion is a force counteracting the distortion. Thus, as the tube/tube distance is increased from $d_{CNT} = 3.712$, the force between the tubes becomes attractive trying to resist the stretching. At some point, the structure cannot withstand the deformation anymore and yields. This results in a rapid drop of the force. Now the force decreases with increasing distance. As is well-known, for a system where the tubes are allowed to move, this situation would lead to mechanical instability. In fact, all branches of the force curve with a negative force gradient would be mechanically unstable for free nanotubes.

The next mechanically stable state is the repulsive maximum at $d \approx 4.0$. The structure of the system now resembles that at $d_{CNT} = 4.089$. As it is compressed, the force is repulsive.

It is somewhat surprising that the number of particles in the global potential minimum reflects the symmetry of the system, yet there appears to be no particular structuring of the beads in this region that would indicate a link to the structure of the crossing. This is indicated by the local densities in Figure 5a and b. They represent a thick slab of the central aggregate such

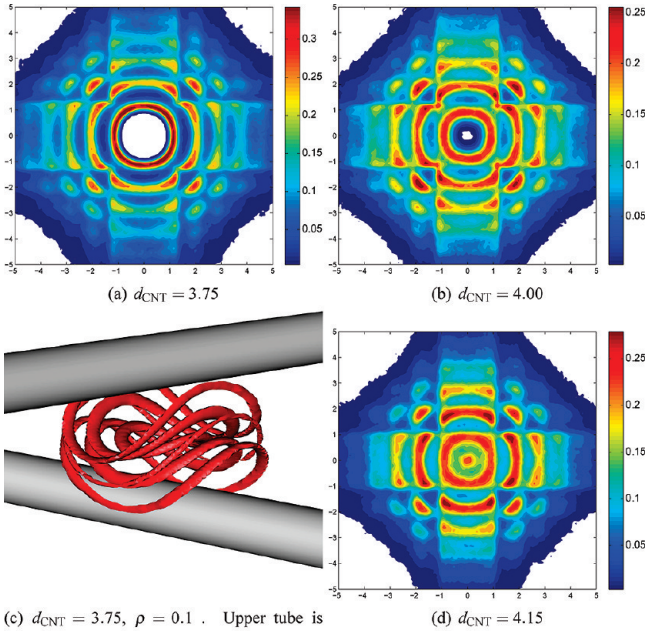

Figure 5. Details of the internal structure of the hydrophobic core of the central aggregate in the regime of high-frequency oscillations: (a, b, d) local density maps for a thick slab incorporating the entire inner torus for different tube/tube distances, as indicated in the figure; (c) like part a but density isosurfaces for $\rho = 0.1$. In part c, the upper tube is slightly offset to allow a better view of the tori structure. Note that no particular structure of the inner torus is visible. The intense structure in the region beyond the inner torus is generated by cutting through the outer tori.

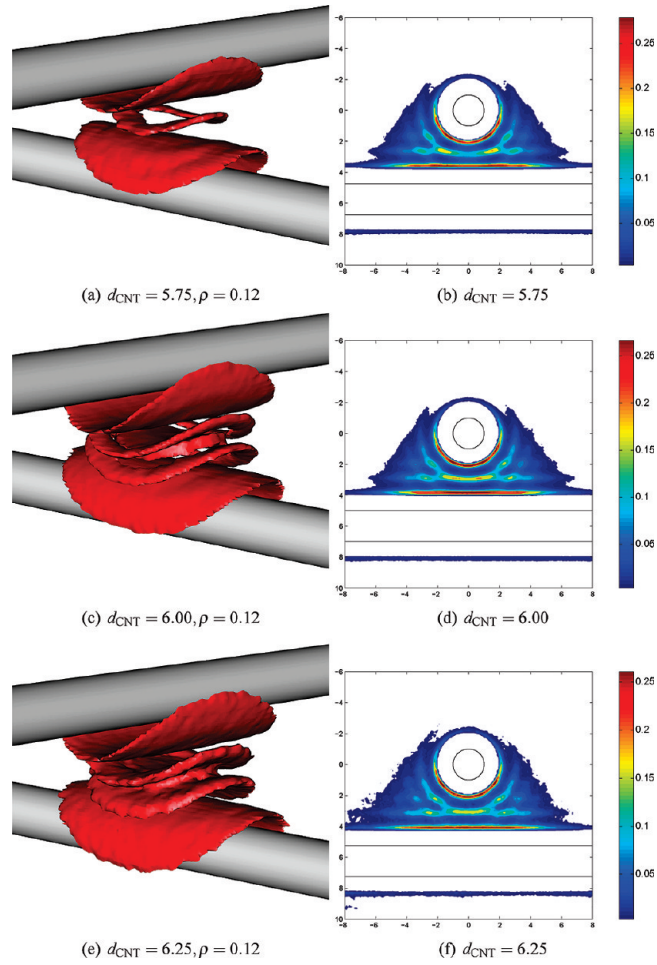

Figure 6. Details of the internal structure of the hydrophobic core of the central aggregate in the layering regime for three distances around the three-layer state: (left column) density isosurfaces for $\rho = 0.12$; (right column) local density maps as in Figure 4. The inner layer forms a hole in the middle when compressed or a bifurcation when stretched. The increasing deformation, i.e., stretching, of the central aggregate with increasing distance between the tubes is visible in the density maps in the right column.

that the entire torus shown in Figure 4e is included. The slab is centered in the center between the tubes and oriented parallel to both tubes. The torus depicted in Figure 4e is clearly visible as an almost perfect circle in the center of Figure 5a. There appears to be significant structuring surrounding the innermost ring of highest density. This is an illusion generated by slab cutting through a number of further tori belonging to regions of high density surrounding the innermost torus (Figure 5c).

Between $d \approx 4$ and $d \approx 7.5$, the force goes through a number of oscillations with a wavelength significantly larger than that of the oscillation between $d \approx 3.7$ and $d \approx 4$. Fitting a damped sin function to this oscillatory region of the force reveals a wavelength of 1.1 which is very close to the location of the bead/bead potential minimum $2^{1/6}$.

Oscillations in force/distance curves have been observed for many confined fluids in theoretical and computer simulation studies[23−26] as well as experimentally.[27,28] They are attributed to layering, i.e., organization of the molecules of the confined fluid into layers parallel to the surfaces. The ordering is induced by the surface/fluid interaction, causing the formation of a dense layer of fluid molecules in the potential minimum. This fluid "surface layer" in turn induces the formation of a second layer. The distance between the first and second layer is equal to the location of the fluid/fluid potential minimum. If the surface layer is located in the minimum of the surface/fluid potential, no forces are exerted on the solid surfaces. If the confined fluid is compressed or stretched by reducing or increasing the distance between the surfaces, the confined fluid responds with a repulsive or attractive force, respectively. When, e.g., the compression becomes too strong, the fluid yields. The stress is released by reducing the number of layers by one layer. The resulting state is very similar to the initial one but consists of one layer less. This leads to the well-known oscillations in the force curve.

The density isosurfaces in Figure 6 reveal the layered structure of the hydrophobic core of the central aggregate around $d \approx 6.0$. As the distance between the CNTs is reduced from $d \approx 6.0$ to $d \approx 4.2$, the number of layers is reduced from three in Figure 6b to one in Figure 5d where the system is shown at the verge of formation of the first layer. Two layers have been "pushed out" during the compression, and the system went through two oscillations in the force curve.

Because of the high curvature of the confining CNTs, the layers are not planar (Figure 6). During compression and stretching, the system undergoes a number of morphological changes. Most striking is the creation of a hole in the center of the middle layer where the confinement is highest (Figure 6a and b). The formation of the fourth layer upon stretching appears to be an essentially continuous process in which the bifurcation, visible in Figure 6e and f, moves to the center of the aggregate.

It is important to realize that hydrophobic beads cannot just be "pushed out", as they belong to surfactant molecules and these molecules belong to a self-assembled aggregate that is larger than the region of confinement. Thus, the only way of

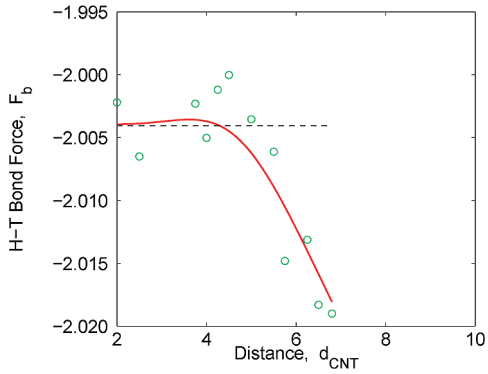

Figure 7. Tube/tube distance dependence of the force exerted by the surfactant head groups on the tail groups along the H−T bond connecting the head to the tail of surfactant molecules in the central aggregate. The horizontal line demarcates the bond stretching force in bulk micelles. Note that for $d_{CNT} \gtrsim 5$ the bond stretching force increases beyond the value found for bulk micelles, indicated by the horizontal line. The solid line is a guide to the eye.

pushing beads out of the region of highest confinement is by deformation of the aggregate. Therefore, the oscillations in the number of molecules in the central aggregate are not as strong as one might expect for confined simple fluids. Most importantly, they do not decrease as the distance between the tubes decreases but increase.

The most striking feature of the force curve is that the surfactant generated force is generally attractive in the region where we observe layering. Following the discussion above, it is clear that this attraction cannot be generated by the layered confined fluid alone, as this would lead to oscillations around $F = 0$. As the system is heterogeneous, a surface tension could have the observed effect. The attractive force would be the result of the tendency of the system to reduce the number of molecules in the interface. However, on the contrary, we observe an increase of the number of molecules in the central aggregate with decreasing tube/tube distance, suggesting an increase in the size of the interface.

To identify the reason for the attractive interaction, let us assume a system with three layers similar to the one shown in Figure 6c. Let us further assume that all layers are located in the respective bead/CNT and bead/bead potentials. The surfactant/CNT force of this system would be zero. (The forceless state is actually slightly different, as the middle layer is in the attractive range of the bead/CNT potential, but we can ignore this for the moment—a system with two layers would not have this contribution.) In order to cause an attraction between the tubes, there must be a constant force trying to pull the beads out of the bead/CNT potential minimum into the attractive region.

The only possible sources of this force are the surfactant head groups. The existence of the pulling force can be proven by calculating the average force stretching the bond that connects the head and tail parts of the surfactant molecules. The result is presented in Figure 7. The bond force is always attractive, meaning that the heads pull on the tails. Initially, it has approximately the same value as that in bulk micelles. In this case, the pulling is compensated by the attractions between tail beads. If we assume the same to be true for the adsorbed micelle, constituting the central aggregate, the pulling of the head groups is compensated by the attraction of the tails alone. As the distance between the tubes increases to $d \approx 5$ and beyond, the bond stretching force increases rapidly. This increase in the force must be compensated by the interaction between the surfactant tail beads and the CNTs.

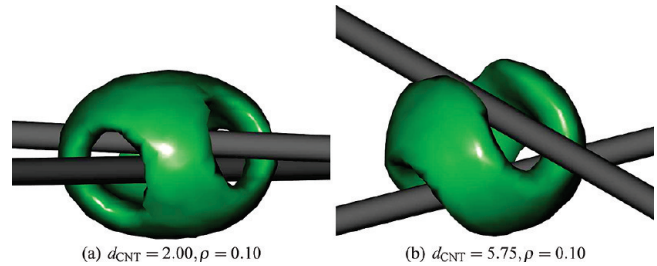

(a) $d_{CNT} = 2.00, \rho = 0.10$ (b) $d_{CNT} = 5.75, \rho = 0.10$

Figure 8. Density isosurfaces $\rho = 0.10$ for the hydrophilic head groups showing the increased confinement with increasing tube/tube distance.

Comparison of Figures 4b and 6e and f indicates that at larger tube/tube separations the hydrophobic core of the central aggregate becomes more and more cylindrical. This means that the heads pull essentially perpendicular to the axis of the central aggregate. This can only create a force component acting on the nanotubes and pointing in the z-direction because the tube surfaces are curved. Applying the same arguments detailed to explain the repulsive region $2 \lesssim d \lesssim 3.7$ leads to the conclusion that the additional pulling from the head groups leads to an effective attraction between the tubes.

This leaves the question about the origin of the force exerted by the head groups. As the distance between the tubes increases from $d_{CNT} = 2.00$ to $d \approx 7.5$, the central aggregate is deformed from an essentially spherical shape to a cylindrical shape. The initial spherical shape is similar to that of bulk micelles. The high curvature provides room for the head groups to move, although they are already feeling the confinement and pull on the interface. As the shape becomes more and more cylindrical, head groups are becoming more and more confined (Figure 8). This increased degree of confinement causes some of the molecules to leave the central aggregate (Figure 2b), while the remaining head groups pull more strongly on the tails (Figure 7). It is interesting to note that, because the attractive force between the tubes is caused by mutual repulsion of surfactant head groups, it is entropic in nature.

Conclusions

Surfactants adsorb and aggregate on crossing carbon nanotubes at concentrations well below the CMC. If the concentration is chosen well, self-assembly occurs only at the crossing where a central aggregate is formed. At small distances between the CNTs, this central aggregate resembles a bulk micelle.[7]

The results of the present study show that a central aggregate is formed as long as the tube/tube distance is not larger than $d \approx 7.5$. In other words, the aggregate is not formed if the gap between the surfaces of the tubes is larger than the diameter of the hydrophobic core of a bulk micelle[7] which is around 5.

The surfactants in the central aggregate interact with the tubes and create an effective force between them. The dependence of the force on the tube/tube separation is very rich. The key features are: (i) At small separations, the force is repulsive as surfactant tail beads are drawn to the tubes by the strong hydrophobic-bead/CNT interaction. (ii) As molecules move into the gap between the tubes, strong layering is observed, creating the well-known oscillations in the force. Just before a single layer is formed, correlations of beads located in the global bead/CNT potential minimum cause additional oscillations at higher frequencies. (iii) The central aggregate disappears at $d \approx 7.5$, and no force is observed at $d \gtrsim 7.5$. (iv) Most importantly, the surfactants create a large attractive region between $d \approx 4$ and the rupturing distance. This attraction is entropic in nature and

caused by the deformation of the central aggregate and the resulting confinement of the head groups.

The latter observation is most important for the bottom-up design of CNT composite materials: (i) It is possible to direct adsorption and self-assembly to the CNT crossings. (ii) The tubes need to be near each other but do not have to touch. (iii) The aggregate pulls the tube together and, thus, stabilizes their target structure.

Acknowledgment. P.A. would like to thank the EPSRC and the Chemical Enginering Endowment Fund for financial support. S.A.H. would like to thank Oman and Emirates Investment Holding Company for financial support.

References and Notes

(1) Strey, R. *Ber. Bunsen-Ges.* **1996**, *100*, 182–182.
(2) Futterer, T.; Hellweg, T.; Findenegg, G. H.; Frahn, J.; Schluter, A. D. *Macromolecules* **2005**, *38*, 7443–7450.
(3) Tanford, C. *Proc. Natl. Acad. Sci. U.S.A.* **1974**, *71*, 1811–1815.
(4) Larson, R. *J. Phys. II* **1996**, *6*, 1441–1463.
(5) Chennamsetty, N.; Bock, H.; Scanu, L. F.; Siperstein, F. R.; Gubbins, K. E. *J. Chem. Phys.* **2005**, *122*, 094710.
(6) Steitz, R.; Muller-Buschbaum, P.; Schemmel, S.; Cubitt, R.; Findenegg, G. H. *Europhys. Lett.* **2004**, *67*, 962–968.
(7) Angelikopoulos, P.; Bock, H. *J. Phys. Chem. B* **2008**, *112*, 13793–13801.
(8) Shvartzman-Cohen, R.; Florent, M.; Goldfarb, D.; Szleifer, I.; Yerushalmi-Rozen, R. *Langmuir* **2008**, *24*, 4625–4632.
(9) Findenegg, G.; Eltekov, A. *J. Chromatogr., A* **2007**, *1150*, 236–240.
(10) Dietsch, O.; Eltekov, A.; Bock, H.; Gubbins, K. E.; Findenegg, G. H. *J. Phys. Chem. C* **2007**, *111*, 16045–16054.
(11) Bock, H.; Gubbins, K. E. *Phys. Rev. Lett.* **2004**, *92*, 135701.
(12) Wallace, E.; Sansom, M. *Nano Lett.* **2007**, *7*, 1923–1928.
(13) Wallace, E. J.; Sansom, M. S. P. *Nanotechnology* **2009**, *20*, 045101.
(14) O'Connell, M. J.; Boul, P.; Ericson, L. M.; Huffman, C.; Wang, Y.; Haroz, E.; Kuper, C.; Tour, J.; Ausman, K. D.; Smalley, R. E. *Chem. Phys. Lett.* **2001**, *342*, 265–271.
(15) Schroder, E.; Hyldgaard, P. *Mater. Sci. Eng., C* **2003**, *23*, 721–725.
(16) Kleis, J.; Hyldgaard, P.; Schrï£!der, E. *Comput. Mater. Sci.* **2005**, *33*, 192–199.
(17) Girifalco, L. A.; Hodak, M.; Lee, R. S. *Phys. Rev. B* **2000**, *62*, 13104–13110.
(18) Muller, E. A.; Rull, L. F.; Vega, L. F.; Gubbins, K. E. *J. Phys. Chem.* **1996**, *100*, 1189–1196.
(19) Walther, J. H.; Jaffe, R. L.; Kotsalis, E. M.; Werder, T.; Halicioglu, T.; Koumoutsakos, P. *Carbon* **2004**, *42*, 1185–1194.
(20) Weisstein, E. W. http://mathworld.wolfram.com/Point-LineDistance3-Dimensional.html.
(21) Groot, R. D.; Warren, P. B. *J. Chem. Phys.* **1997**, *107*, 4423–4435.
(22) Matsumoto, M.; Nishimura, T. *ACM Trans. Model. Comput. Simul.* **1998**, *8*, 3–30.
(23) Tang, Z.; Scriven, L. E.; Davis, H. T. *J. Chem. Phys.* **1994**, *100*, 4527–4530.
(24) Bock, H.; Schoen, M. *J. Phys.: Condens. Matter* **2000**, *12*, 1545–1568.
(25) Klapp, S. H. L.; Schoen, M. *J. Chem. Phys.* **2002**, *117*, 8050–8062.
(26) Bock, H.; Gubbins, K. E.; Ayappa, K. G. *J. Chem. Phys.* **2005**, *122*, 094709.
(27) Klapp, S. H. L.; Grandner, S.; Zeng, Y.; von Klitzing, R. *J. Phys.: Condens. Matter* **2008**, *20*, 494232–494238.
(28) Heuberger, M.; Zäch, M.; Spencer, N. D. *Science* **2001**, *292*, 905–908.

JP903121A